

1 **Running Title : *OsLUGL* regulating floral development through auxin**
2 **pathway**

3 **Chunyan Yang • Dianli Li • Xingjie Zhu • Ziyao Wei • Zhiming Feng • Long Zhang • Jun He**
4 **• Xi Liu • Changling Mou • Ling Jiang ^(✉) and Jianmin Wan ^(✉)**

5

6 ***OsLUGL* involved in floral development through regulating auxin**
7 **level and *OsARFs* expression in rice (*Oryza sativa* L.)**

8

9 **C.Y. Yang¹ • D.L. Li¹ • X.J. Zhu¹ • Z.Y. Wei¹ • Z.M. Feng¹ • L. Zhang¹ • J. He¹ • X. Liu¹ •**

10 **C.L. Mou¹ • L. Jiang^{1, †} • J.M. Wan^{1,2, †}**

11

12 ¹*State Key Laboratory for Crop Genetics and Germplasm Enhancement, Jiangsu Plant Gene Engineering*
13 *Research Center, Nanjing Agricultural University, Nanjing 210095, China, and*

14 ²*National Key Facility for Crop Resources and Genetic Improvement, Institute of Crop Science, Chinese Academy*
15 *of Agricultural Sciences, Beijing 100081, China*

16

17 † Corresponding authors:

18 Ling Jiang

19 Telephone: +86-25-84399061

20 Fax: +86-25-84399061

21 E-mail: jiangling@njau.edu.cn

22 ORCID iD: <https://orcid.org/0000-0003-1464-5881>

23

24 Jianmin Wan

25 Telephone: +86-25-84396516

26 Fax: +86-25-84396516

27 E-mail: wanjm@njau.edu.cn

28 ORCID iD: <https://orcid.org/0000-0002-7813-4362>

29

30 **Highlight**

31 OsLUGL through forming OsLUGL-OsSEU-OsAP1-OsSEP3 complex regulate
32 *OsGH3-8* expression, and regulate auxin level and *OsARFs* expression indirectly. This
33 work is a new insight to floral development molecular mechanism.

34

35 **Abstract**

36 Specification of floral organ identity is critical for floral morphology and
37 inflorescence architecture. Floral organ identity in plants is controlled by floral
38 homeotic A/B/C/D/E-class genes. Although multiple genes regulate floral
39 organogenesis our understanding of the regulatory network remains fragmentary. Here,
40 we characterized rice floral organ gene *KAIKOUXIAO* (*KKX*), mutation of which
41 produces an uncharacteristic open hull, abnormal seed, and semi-sterility. *KKX*
42 encodes a putative LEUNIG-like (LUGL) transcriptional co-repressor. *OsLUGL* is
43 preferentially expressed in young panicles and its protein can interact with OsSEU,
44 which functions were reported as an adaptor for LEUNIG. OsLUGL-OsSEU
45 functions together as a transcriptional regulatory complex to control organ identity
46 specification through regulation of MADS-box genes. During this process, SEP3
47 (such as OsMADS8) and AP1 (such as OsMADS18) serve as the DNA-binding
48 partner of OsLUGL-OsSEU complex. Further studies indicated that OsMADS8 and
49 OsMADS18 could bind the promoter of *OsGH3-8* and regulate its expression. The
50 altered expression of *OsGH3-8* caused the increased auxin level and the decreased
51 expression of *OsARFs*. Overall, our results demonstrate a possible pathway whereby
52 OsLUGL-OsSEU-OsAP1-OsSEP3 complex as a transcriptional regulator by targeting
53 the promoter of *OsGH3-8* directly, affecting auxin level, *OsARFs* expression level and
54 thereby influencing floral development. These findings provide a valuable insight into
55 the molecular functions of OsLUGL in rice floral development.

56

57 **Key words:** rice, OsLUGL, *OsGH*, OsMADSs, floral development, Auxin, *OsARFs*

58

59 Introduction

60 Rice (*Oryza sativa* L.) as one of the most important cereal crops feeds more than half
61 the world population. Given the rapidly increasing population and decreasing
62 cultivated land area, continued improvements in rice production and quality are
63 massive challenges for rice breeders (Ikeda *et al.*, 2013). Normal development of
64 floral organs in rice is essential for reproduction and seed quality (Zhang *et al.*, 2015).
65 Initiation and differentiation of floral organs are of fundamentally important in the
66 plant life cycle (Zhang *et al.*, 2007; Fornara *et al.*, 2010). A typical dicot flower
67 consists of four whorls, intensive molecular and genetic analyses in *Arabidopsis*
68 *thaliana* and *Antirrhinum majus*, led to the ABCDE model (Coen and Meyerowitz,
69 1991; Alvarez-Buylla *et al.*, 2010; Litt and Kramer, 2010). The functions of
70 A/B/C/D/E are to specify the identity of each organ and to control floral meristem
71 determinacy (Coen and Meyerowitz, 1991; Pelaz *et al.*, 2000; Theissen and Saedler,
72 2001; Pinyopich *et al.*, 2003; Ditta *et al.*, 2004). Rice is a monocot grass species and
73 the model plant for functional genomics studies in crop plants; its spikelet
74 morphogenesis is important for the achievement of yield. Accumulating evidence
75 shows that the ABCDE model is at least partially applicable to floral development in
76 rice (Ferrario *et al.*, 2004; Bommert *et al.*, 2005; Thompson and Hake, 2009; Ciaffi *et*
77 *al.*, 2011; Tanaka *et al.*, 2013; Zhang and Yuan, 2014; Wang *et al.*, 2015; Dreni and
78 Zhang, 2016;).

79
80 Many A/B/C/D/E class genes have been identified, and most of them are MADS-box
81 family genes. Five types of MADS-box genes identified in from *Arabidopsis* are
82 partially conserved in rice, and these genes are reported to be involved in specification
83 of floral development. *OsMADS15* is reported as a regulator of palea size (Wang *et al.*,
84 2010); *OsMADS16* regulate development of lodicules and stamens (Yun *et al.*, 2013);
85 *OsMADS3* plays a predominant role in stamen specification, whereas *OsMADS58* is
86 involved in establishing floral meristem determinacy and carpel development (Dreni
87 *et al.*, 2011; Hu *et al.*, 2011); *OsMADS13* has a key role in specification of ovule

88 identity and floral meristem determination (Dreni and Kater, 2014; Hu *et al.*, 2015).

89

90 Rice has diversified at least five *SEP*-like genes that specify the identities of
91 four-whorl floral organs, such as *OsMADS1*, *OsMADS5*, *OsMADS7*, *OsMADS8*, and
92 *OsMADS34* (Malcomber and Kellogg, 2004, 2005; Zahn *et al.*, 2005; Arora *et al.*,
93 2007; Wu *et al.*, 2018). Loss-of-function *OsMADS1* shows the outer floret organs,
94 lemma and palea, were narrow, poorly developed, and failed to enclose the inner
95 organs (Khanday *et al.*, 2013). *osmads7* and *osmads8* exhibit late flowering, homeotic
96 transformations of lodicules, stamens, and carpels into palea/lemma-like organs, and a
97 loss of floral determinacy (Cui *et al.*, 2010). *OsMADS6* is *AGL6*-like gene have high
98 sequence similarities with *SEP*-like genes (Dreni and Zhang, 2016; Callens *et al.*,
99 2018), in *osmads6*, the palea develops five to six vascular bundles, which resembles
100 the identity of a wild-type lemma (Li *et al.*, 2010; Dreni and Zhang, 2016).

101

102 In grass reproductive meristems, the phytohormone auxin plays a central role in
103 almost all developmental and physiological processes, it regulates axillary meristem
104 initiation and outgrowth by controlling cell polarity establishment and cell elongation
105 (Zhao, 2010). Auxin responses are mediated by a class of transcription factors known
106 as *auxin response factors (ARFs)* (Overvoorde *et al.*, 2005; Boer *et al.*, 2014). The
107 functions of *ARFs* are well studied. Many loss-of-function mutations affecting floral
108 morphology have been reported in *Arabidopsis thaliana*. For example, *arf1* and *arf2*
109 affect leaf senescence and floral organ abscission (Ellis *et al.*, 2005); *arf3* displays
110 defects in the gynoecium and floral meristem patterning (Nishimura *et al.*, 2005;
111 Zheng *et al.*, 2018). In rice, the transgenic lines expressing an antisense *OsARF1*
112 showed extremely slow growth, poor vigor, curled leaves, and sterility (Attia *et al.*,
113 2009). Mutation of *OsARF19* caused abnormal floral organs, and changes to plant
114 height, leaf shape, and seed size (Zhang *et al.*, 2015).

115

116 *Arabidopsis* LUG was Gro/Tup1-like co-repressor identified in plants; its role is to
117 regulate transcription of the floral homeotic gene *AGAMOUS (AG)* (Conner and Liu,

118 2000). In loss-of-function mutants of LUG, *AG* is ectopically expressed in the outer
119 two whorls of the flower, converting sepals into carpelloid floral organs and reducing
120 the numbers of petals and stamens (Liu and Meyerowitz, 1995). Like other Gro
121 family members, the N-terminal LUGS domain of LUG is required for repression of
122 transcription and for direct interaction with SEUSS (SEU), SEU acts as an adaptor
123 protein, bridging interaction between LUG and specific DNA-binding transcription
124 factors AP1 and SEP3. The LUG-SEU-AP1-SEP3 complex is directly regulating *AG*
125 expression in all four whorls in *Arabidopsis* (Sridhar *et al.*, 2004; Gregis *et al.*, 2006;
126 Sridhar *et al.*, 2006; Sitaraman *et al.*, 2008; Gregis *et al.*, 2009). There is no report on
127 LUG or its regulatory mechanism in rice.

128

129 Here, we characterize rice floral organ gene *KAIKOUXIAO (KKX)*, mutation of which
130 causes an uncharacteristic open glume and abnormal seed. *KKX* encodes a putative
131 LEUNIG-like (LUGL) transcriptional co-repressor. Further analyses revealed that
132 OsLUGL interacts with OsSEU to become a transcriptional regulated complex.
133 OsSEU also interacts with OsMADS8 and OsMADS18. Also, we confirmed that
134 *OsGH3-8* is the downstream target of OsMADS8 and OsMADS18. In *kcx*, the
135 down-regulated expression of *OsGH3-8* cause high auxin level and altered *OsARFs*
136 expression. Thus, our results suggest that OsLUGL regulates floral organ
137 development by forming OsLUGL-OsSEU-OsAP1-OsSEP3 complex, which could
138 regulate auxin level and signaling directly.

139

140 **Materials and methods**

141 *Plant materials*

142 The *kkx* mutant was from a M₂ population of ⁶⁰Co-irradiated variety Nanjing35
143 (*Oryza sativa*, L.). The *kkx* was crossed with crossed with the typical *indica* cultivar
144 93-11 to construct the mapping population. The F₁ seeds of *kkx*×93-11 were sown and
145 transplanted as individual plants to generate the F₂ plants for gene mapping.
146 Nanjing35 was used as the wild-type plants for phenotypic analysis. All plants were
147 cultivated in an experimental field under natural long-day conditions in Nanjing,
148 China.

149

150 *Fertility evaluation of pollen and embryo sac*

151 Ten individuals from wild-type and *kkx* were examined to determine the pollen
152 fertility. Ten florets from three panicles of each plant were collected 2-3 hours before
153 flowering. All anthers per floret was mixed, placed on the slide, mashed, and stained
154 with 1% iodine potassium iodide (I₂-KI) solution, and observed with an ECLIPS E80i
155 (Nikon, Tokyo, Japan) light microscope.

156 To observe the embryo sac development of the wild-type and *kkx*, spikelets were
157 collected immediately after pollens disperse, fixed in FAA solution. Before staining,
158 remove lemma, palea and anthers. The embryo sac was then processed through an
159 ethanol series (70%, 50% and 30%) and finally transferred into distilled water (30 min
160 each). The whole ovary was incubated in 2% aluminum potassium sulfate (KAl
161 (SO₄)₂) water solution for 30 min, then held in eosin Y water solution for 10-12 h, and
162 then in 2% aluminum potassium sulfate for 20 min, after washing 2-3 times with
163 distilled water. The ovaries were processed through an ethanol series (30%, 50%, 70%,
164 80%, 90%, 100% and 100%, 30 min each), then transitted to a mixture of absolute
165 ethyl alcohol and methyl salicylate (1:1) for 1-2 h, the held in methyl salicylate over
166 12 h. Fertility of embryo sacs was examined by confocal laser scanning microscopy
167 (Leica SP8).

168

169 *Microscopy observations*

170 For paraffin sectioning, *kkx* and wild-type flowers from young panicles were fixed in
171 formalin–acetic acid–alcohol (FAA) solution, and samples were treated by a graded
172 series of dehydration and infiltration steps. Fixed tissues were embedded in paraplast.
173 Samples were sectioned to 15 μm , stained with 0.1% toluidine blue and observed with
174 an ECLIPS E80i (Nikon, Tokyo, Japan) light microscope.

175 For scanning electron microscopy (SEM), young panicles were fixed in 2.5% (v/v)
176 glutaraldehyde, and fixed overnight at 4°C after vacuuming, and dehydrated through a
177 graded concentration of ethanol. The samples infiltrated and embedded in butyl
178 methyl methacrylate, treated with critical point drying, and then sputter coated with
179 platinum. All tissues were observed with HITACHI S-3000N scanning electron
180 microscope.

181

182 *Gene mapping and RNAi suppression of the KKK gene*

183 83 plants with *kkx* phenotypic were selected from the F₂ mapping population of *kkx*
184 and 93-11 for preliminary mapping using 122 polymorphic SSR (simple sequence
185 repeat) markers between *kkx* and 93-11. Then, 513 F₂ recessive plants were used for
186 fine mapping. Fine-mapping sequence-tagged site primers were designed according to
187 the different DNA sequences of 93-11 and Nipponbare (*O. sativa*, *japonica*.) obtained
188 from the National Center for Biotechnology Information (NCBI). Primers used for
189 mapping are listed in Supplementary Table S1.

190 To obtain *KKX* RNAi plants, the construct LH-1390-RNAi was used as an RNAi
191 vector. Both sense and antisense versions of a specific 200 bp fragment from the
192 cDNA of *KKX* were amplified with primer pairs *KKX*-RNAi-L and *KKX*-RNAi-R
193 (Supplementary Table S2), and cloned into LH-1390-RNAi to create the
194 *dsRNAiOsKKX* construct, which was then transformed into the rice variety Nanjing35
195 by the *Agrobacterium*-mediated method (Hiei *et al.*, 1994).

196

197 *Real-time PCR analysis*

198 Total RNA from seedling, root, shoot, leaf, panicle, young spikelet, and different stage

199 of panicles were isolated using the RNA prep Pure Plant Kit (TIANGEN, Beijing,
200 China). First-strand cDNA was reverse transcribed from 1µg of total RNA using the
201 PrimeScript 1st Strand cDNA Synthesis Kit (TaKaRa). Rice ubiquitin (UBQ) was
202 used as endogenous control. Real-time PCR was performed using a SYBR Premix Ex
203 Taq™ kit (TaKaRa) on an ABI prism 7500 real-time PCR System and three
204 biological repeats. Primers used for real-time PCR analysis are listed in
205 Supplementary Table S3.

206

207 *Subcellular localization of LUGL*

208 To explore the subcellular localization of OsLUGL, the C-terminus of OsLUGL
209 cDNA was fused with green fluorescent protein (GFP) and inserted in the pAN580
210 vector between the d35S promoter and the nopaline synthase (NOS) terminator. In
211 addition, we used the mCherry-tagged rice prolamin box binding facto
212 (RPBF-mCherry) vector as a nuclear marker (Kawakatsu *et al.*, 2009). And the
213 35s-OsLUGL-GFP plasmid and the nuclear marker plasmid were co-transformed into
214 rice protoplasts. Rice protoplasts were prepared, transfected, and cultured as
215 previously described (Wang *et al.*, 2016). Fluorescence images were observed using a
216 Zeiss LSM510. Primers used to make subcellular localization constructs are listed in
217 Supplementary Table S2.

218

219 *RNA in situ hybridization*

220 RNA in situ hybridization was performed as described previously (Chen *et al.*,
221 2015) with minor modifications. The young panicles of all stages from Nipponbare (*O.*
222 *sativa*, *japonica*.) was fixed in FAA solution, subjected to a dehydration series and
223 infiltration, and embedded in paraplast and sectioned at 8µm using a Leica RM2235
224 microtome. A 360 bp gene-specific region of OsLUGL amplified with primers
225 OsLUGL-PF and OsLUGL-PR (see Supplementary Table S2) was cloned into the
226 pGEM-T Easy vector (Promega). The linearized templates were amplified from the
227 pGEM-T plasmid containing the gene-specific region of SLG using primers Yt7 and
228 Ysp6. Digoxigenin-labeled RNA probes were prepared using a DIG Northern starter

229 kit (Cat. No. 2039672, Roche) following the manufacturer's instructions. Slides were
230 observed under bright field using a Leica DM5000B microscope.

231

232 *Yeast two-hybrid assay*

233 The yeast two-hybrid assays were performed using the Matchmaker Yeast
234 Two-Hybrid System (Clontech). Various fragments from OsLUGL^{WT} and OsLUGL^{kkx}
235 were cloned into pGBKT7, and OsSEU was cloned into pGADT7. All constructs were
236 transformed into the recipient strain AH109 and selected on SD/-Trp-Leu (DDO)
237 plates at 30°C for 2-3 days. The interactions were assayed on selective medium
238 SD/-Trp-Leu-His-Ade (QDO) plates at 30°C for 3-5 days. For testing the interaction
239 with OsMADSs, full-length cDNA of OsMADS8/14/15/18 were cloned into pGBKT7,
240 and full-length cDNA of OsMADS6/14/15/18 were cloned into pGADT7. All
241 constructs and/or OsSEU-AD were transformed into the recipient strain AH109 and
242 selected as mentioned above. Primers used to make these construct are listed in
243 Supplementary Table S2.

244

245 *Bimolecular fluorescence complementation (BiFC) assay*

246 Full-length cDNA of OsLUGL^{WT} and OsLUGL^{kkx} were cloned into the p2YN (eYFP)
247 vector to construct the OsLUGL^{WT}-eYFPN fusion protein and OsLUGL^{kkx}-eYFPN
248 fusion protein, respectively. OsSEU was cloned into the p2YC (eYFP) vector to
249 produce OsSEU-eYFPC fusion proteins. Primers used to make these constructs are
250 listed in Supplementary Table S2. These plasmids were co-expressed in tobacco leaf
251 epidermis cells by *Agrobacterium*-mediated infiltration (Hiei *et al.*, 1994). The
252 mCherry ER-rk CD3-959 was used as ER (endoplasmic reticulum) marker (Nelson *et*
253 *al.*, 2007). Yellow fluorescent protein was observed using a Zeiss LSM510 after 48 h
254 infiltration.

255

256 *Transactivation analysis*

257 The full-length OsSEU was fused to the GAL4 DNA BD-coding (Yeast Two-hybrid
258 System, Clontech) sequence and constructed into pAN580, which was cutoff GFP

259 protein, to generate effector plasmid pAN580-GAL4-OsSEU. The full-length
260 OsLUGL^{WT} was fused into the pAN580 (no GFP) to generate effector plasmids
261 pAN580- OsLUGL^{WT}. The reporter was a plasmid harbouring firefly LUC (luciferase)
262 gene which was controlled by a modified 35S promoter with 5× the UAS (upstream
263 activating sequence) in it. pRT107 vector containing the BD sequence and BD-VP16
264 fusion sequence were used as negative and positive control respectively. A pPTRL
265 plasmid that contained a CaMV (Cauliflower mosaic virus) 35S promoter and Renilla
266 LUC, was used as an internal control (Ohta *et al.*, 2000). To test the transactivation of
267 OsMADSs, full-length cDNA of OsMADS8/18 were fused into pAN580 (no GFP) to
268 generate effector. To generate the pOsGH3-8:LUC reporter construct, ~ 2 kb of the
269 OsGH3-8 promoter was cloned into pGreenII-0800-LUC. The different effectors and
270 different reporters were co-transformed into rice protoplasts in different combinations.
271 Rice protoplasts were prepared as mentioned before. The luciferase activity assay was
272 investigated using the dual luciferase reporter assay system and the relative luciferase
273 activity was detected referring to the protocol (Promega, E1910). The primers used
274 for the constructions are listed in Table S2.

275

276 *Yeast one- hybrid assay*

277 For yeast one-hybrid assays, the full length cDNA of OsMADS8/18 were cloned into
278 pB42AD vector, and promoter of OsGH3-8 was fused into pLacZi vector. Plasmids
279 were co-transformed into yeast strain EGY48 according to the manufacturer's manual
280 (Clontech). Transformed yeast was plated onto a synthetic medium DDO (-Ura/-Trp).
281 Positive transformants was screened by adding 80 mg·L⁻¹ X-α-gal into SD/-Ura/-Trp
282 medium. The primers used for the constructions are listed in Table S2.

283

284 **Results**

285 *Phenotypic characterization of *kkx**

286 To investigate the regulation of rice floral development, we identified floral mutant
287 *kkx*, which has displays open hulls, semi-sterile, smaller anthers and pistils, and poor
288 quality seeds (Figure 1a-e). I₂-KI staining showed normal pollen fertility (Figure 1f,
289 g). Also, observation of the embryo sacs showed that normal embryo sacs in wild-type
290 and *kkx*, of which two polar nuclei located in the central cavity with horizontal
291 arrangement instead of vertical one (Figure S1). In terms of agronomic traits
292 1,000-grain weight was significantly reduced, and seed set was $57.50 \pm 6.40\%$
293 compared to wild-type at $82.78 \pm 6.63\%$. Plant height and panicle length were similar
294 to wild-type (Figure S1).

295

296 *The *kkx* mutant shows open glumes*

297 The lemma and palea of wild-type florets form an interlocked structure with two
298 hamuli at the marginal regions of the palea (mrp) (Figure 1b and Figure 2a-c). In *kkx*,
299 the abnormally shaped palea cannot interlock with the lemma because of lacking or
300 incomplete hamulus in mrp (Figure 1b and Figure 2d-f). Both wild-type and *kkx* have
301 five vascular bundles in the lemma and three in palea (Figure 2a and d).

302 We analyzed the early spikelets of wild-type and *kkx* using scanning electron
303 microscopy (SEM). At late stage Sp6 (the stamen primordial formation stage), palea
304 primordia were already formed and the stamen primordia were initiated both in
305 wild-type and *kkx* (Figure 2g and k). At early stage Sp7 and stage Sp7 (pistil
306 primordium formation stage), the pistil primordium formed in the center of the six
307 stamens. The developmental processes of stamen were not significantly different
308 between wild-type and *kkx*, but there was a bulge on palea of *kkx*, which marked with
309 white square (Figure 2h, i, l and m). At stage Sp8 (the ovule and pollen formation
310 stage), wild-type and *kkx* formed a normal spikelet, whereas *kkx* had a larger spacing
311 between the lemma and palea (Figure 2j and n). SEM analysis revealed that both the
312 inner and outer epidermal cells of lemma and palea in *kkx* were similar to those of

313 wild-type (Figure S3).

314

315 *OsKXX encodes a putative LEUNIG-Like (LUGL) transcriptional co-repressors*

316 An F₂ population from a cross of the *kkx* mutant and wild-type segregated 151
317 individuals with wild-type phenotype and 38 individuals with mutant phenotype, the
318 segregation ratio was consistent with that expected a single locus ($\chi^2_{3:1} = 0.418$,
319 $P_{1df} > 0.05$). We selected 83 individuals with *kkx* phenotype from the F₂ progeny of a
320 cross between *kkx* and 93-11 and mapped the locus in a region between InDel marker
321 InDelB and SSR marker RM5496 on the long arm of chromosome 1. Further fine
322 mapping narrowed this region to a 36.8 kb genomic region (Figure 3a and b).
323 According to the Rice Genome Automated Annotation System (RiceGAAS,
324 <http://ricegaas.dna.affrc.go.jp>) there were three putative genes in this region, coding
325 for one pentatricopeptide protein, and two *LEUNIG-like (LUGL)* transcriptional
326 co-repressors (Figure 3c).

327 We chose the two *LEUNIG* genes, *LOC_Os01g042260* and *LOC_Os01g042270* as
328 potential candidates. Gene expression profiles analyzed on the Rice Expression
329 Profile Database (RiceXPro, <http://ricexpro.dna.affrc.go.jp/>) indicated that
330 *LOC_Os01g042270* was barely expressed in young inflorescences, and we also could
331 not obtain a PCR product from cDNA extracted from young inflorescences (20 mm)
332 (Figure S4). *LOC_Os01g042260* was chosen for further analysis, which encoding a
333 95.8 kD protein with 876 amino acids, containing three parts, an N-terminal LUF5
334 domain, a central Q-rich domain, and a C-terminal with 7 WD40 repeats (Figure 3d).
335 Sequencing results revealed that the gene in *kkx* had a T deleted in the fifth WD40
336 repeat, resulting in an S779 to L779 transition and a premature stop codon (Figure 3d,
337 and Figure S5).

338 To confirm that the deletion in *LOC_Os01g042260* was responsible for the
339 uncharacteristic open floret phenotype of the *kkx* mutant, we generated transgenic
340 plants carrying a *LOC_Os01g042260* RNA interference (*RNAi*) construct. A plasmid
341 containing two 200 bp fragments of wild-type *LOC_Os01g042260* cDNA inserted
342 forward and reverse into an *LH-1390-RNAi* vector was introduced into rice cv.

343 Nanjing 35. Compared to wild-type, positive lines *RNAi-4* and *RNAi-6* showed open
344 florets and had significantly reduced transcripts of *LOC_Os01g042260* (Figure 3e-g).
345 Anatomical observations revealed that lemmas and paleas of *RNAi-4* and *RNAi-6*
346 were unlocked (Figure 4e, h-k). These results confirmed that *LOC_Os01g042260*
347 (*OsLUGL*) was the *KKX* gene.

348

349 *OsLUGL* was localized in the nucleus and strongly expressed in young panicles

350 To determine the subcellular localization of *OsLUGL*, we fused *OsLUGL* with green
351 fluorescent protein (GFP) at its C-terminus. Transient expression of this fusion protein
352 in rice protoplasts revealed GFP signals in the nucleus (Figure 4a). RT-PCR analysis
353 showed that *OsLUGL* was expressed in all tissues, and strongly in young panicles.
354 Furthermore, *OsLUGL* was most highly expressed during early panicle development,
355 but expression dropped dramatically once the spikelets reached 0.5 cm (Figure 4b).
356 We also performed in-situ hybridization to localize *OsLUGL* expression during early
357 panicle development. Strong expression was detected in spikelet meristem primordia,
358 floral meristem primordia, lemma and palea primordia, and vascular regions (Figure
359 4c). The results of both RT-PCR analysis and in-situ hybridization implied a role of
360 *OsLUGL* in floral organ development.

361

362 *OsLUGL* interacts with *OsSEU* and is required by *OsSEU* to regulate transcription in
363 *planta*

364 Phylogenetic and protein structure analysis found that *OsLUGL* had high homology,
365 especially the LUFS domain in 15 plants (Figure S6 and S7), and in *Arabidopsis*, the
366 protein At4g32551 was reported that it needs an adaptor protein SEU to form a
367 complex to function as a transcriptional regulator (Sridhar *et al.*, 2004). To investigate
368 the functional forms of *OsLUGL*, the full-length and different truncated *OsLUGL*
369 proteins were used for interaction analysis. As shown in Figure 5a, the LUFS domain
370 in the N-terminus of *OsLUGL* was required for interacting with *OsSEU* both in
371 wild-type and *kkx*, but Q-rich domain and WD40 repeats were not affect their
372 interaction. And the ability of this interaction was no significantly different between

373 the wild-type and the *kkx* mutant (Figure 5b). In addition, BiFC analysis also showed
374 that OsLUGL physically interacted with OsSEU in nucleus (Figure 5c).

375 We next tested whether OsLUGL functioned as a transcription regulator in rice. A
376 transient rice protoplast repression assay was adopted, which 5×UAS GAL4-LUC as
377 reporter. OsSEU was fused to the GAL4 DNA BD-coding sequence and transferred
378 into pAN580 to generate effectors pAN580-SEU (35S::SEU-BD) and using
379 pAN580-GAL4 (35S::GAL4-BD) as a negative control. OsLUGL^{WT} was fused to
380 pAN580 to generate effectors pAN580- LUGL^{WT} (Figure 5d). Rice leaf sheath
381 protoplasts were separately transfected with each plasmid together with the reporter,
382 and LUC expression were quantified. SEU-BD or GAL4-BD alone showed no effect
383 on LUC expression, whereas LUGL^{WT} with SEU-BD significantly reduced LUC
384 expression (Figure 5e). These results confirmed that OsLUGL together with OsSEU
385 functions as a transcriptional regulator in rice.

386

387 *OsSEU interacts with SEP3 and AP1 in rice*

388 In *Arabidopsis*, neither LUG nor SEU possesses a recognizable DNA binding motif,
389 the LUG-SEU complex need DNA-binding factor APETALA1 (AP1) and
390 SEPALLATA3 (SEP3) to mediate transcriptional during flower development. During
391 this process, AP1 and SEP3 need to interact with SEU (Sridhar *et al.*, 2006; Sitaraman
392 *et al.*, 2008). Then, we tested whether AP1 and SEP3 serve as the DNA-binding
393 partners of OsLUGL-OsSEU in rice. To determine AP1 or SEP3 that interacts with
394 OsSEU, we performed a yeast two-hybrid assay. OsMADS14, OsMADS15 and
395 OsMADS18 are orthologs of *Arabidopsis* AP1, and OsMADS8 is an ortholog of
396 SEP3 in *Arabidopsis*. OsSEU interacted strongly with OsMADS8 and OsMADS18,
397 but failed to interact with OsMADS14 or OsMADS15 (Figure 5f). These results
398 indicated that OsSEU interact with SEP3 and AP1 in rice.

399

400 *Altered expression of floral organ identity genes in *kkx**

401 To further understand the function of OsLUGL, we tested the expression of
402 A/B/C/D/E class genes. In real-time PCR analysis, A-class (*OsMADS14/18*), B-class

403 (*OsMADS2* and *OsMADS16*), C-class (*OsMADS3/58*) were down-regulated in *kcx*
404 inflorescences (15 mm); A-class (*OsMADS15*) was up-regulated; E-class
405 (*OsMADS7/8/34/57*) genes were down-regulated; E-class (*OsMADS22/29* and
406 *OsCFO1*) were up-regulated. C-class (*OsDL*) gene, D-class (*OsMADS13*) gene and
407 E-class (*OsMADS16*) genes did not vary (Figure 6). *REPI* is a *CYCLOIDEA*-like
408 gene, *osrep1* shows defects in the palea, but not in lemma (Yuan *et al.*, 2009). In *kcx*,
409 the expression of *OsREPI* was down-regulated (Figure 6a). These results showed that
410 the OsLUGL could regulate the expression of floral organ identity genes in rice.

411

412 *OsLUGL-OsSEU-OsAPI-OsSEP3* complex has regulatory effects on *OsGH3-8*
413 expression, auxin level and auxin signaling pathways

414 The phytohormone auxin plays a central role in almost all developmental processes, it
415 regulates axillary meristem initiation (Zhao, 2010; Habets and Offringa, 2014).
416 *OsGH3-8* (*OsMGH3*) is an auxin negative component in regulating auxin level and
417 activity, *dsRNAiOsMGH3* caused phenotypes consistent with auxin overproduction or
418 activated signaling, such as ectopic rooting from aerial nodes, carpel development,
419 glume form, pollen viability and reduced fertility (Yadav *et al.*, 2011), which similar
420 to the *kcx* mutant. Also, *OsMADS6* is positive regulator for *OsGH3-8* (Prasad *et al.*,
421 2005; Zhang *et al.*, 2010; Yadav *et al.*, 2011) (Figure 7a and b). In *kcx*, the expression
422 of *OsGH3-8* was down-regulated, but no change in *OsMADS6*, so, a question arises
423 here. What causes the down-regulated of *OsGH3-8*? In *Arabidopsis*, neither OsLUGL
424 nor OsSEU regulate genes expression directly, because the absent of DNA-binding
425 domain. The LUG-SEU complex needs AP1 and SEP3 act as bridge to binding DNA
426 downstream. In this study, we confirmed that OsSEU can interact with OsMADS8
427 (SEP3) and OsMADS18 (AP1) (Figure 5f), and OsMADS8 and OsMADS18 have
428 high homogeneous of OsMADS6, so we suspect that *OsGH3-8* is direct target of
429 OsMADS8 and/or OsMADS18, OsLUGL-OsSEU-OsAPI-OsSEP3 complex could
430 regulating *OsGH3-8* directly. To test this hypothesis, we performed yeast one hybrid
431 assays using in vitro-expressed OsMADA8 and OsMADS18. As shown in Figure 7a,
432 both of OsMADS8 and OsMADS18 bound to the *OsGH3-8* promoter. To examine the

433 regulation of OsMADS8/18 on the expression of *OsGH3-8*, as shown in Figure 7b,
434 we performed transient expression assays using ~ 2 kb of the *OsGH3-8* promoter
435 fused with LUC as a reporter, and OsMADS8/18 were expressed under control of 35S
436 promoter as effectors. Various effectors and reporter were transfected together into rice
437 protoplasts in different combinations (Figure 7c). Higher LUC activity was detected
438 when OsMADS8/18 protein was transfected with the reporter construct compared
439 with the internal control. Meanwhile, we found that the LUC activity is higher in
440 which when two effectors (OsMADS8 and OsMADS18) co-transfected with
441 pOsMGH3-8 than that when single effector (OsMADS8 or OsMADS18)
442 co-transfected with pOsMGH3-8. These findings strongly support the hypothesis that
443 OsMADS8 and OsMADS18 regulate *OsGH3-8* by binding the promoter of *OsGH3-8*,
444 and OsMADS8 and OsMADS18 have a superposition effect on regulation.
445 The phenotypes of *dsRNAiOsMGH3* are similar to *OsYUCCA* overexpression
446 transgenic rice. *OsYUCCA* is a rice auxin biosynthetic gene, and the overproduction
447 of auxin in its overexpression transgenic lines is expected (Yamamoto *et al.*, 2007). In
448 *kxx*, we found the expression of *OsYUCCA1* is up-regulated, and raised auxin level
449 (Figure 7d and e). We also analyzed the expression of all *OsARFs* in young
450 inflorescences (15 mm). The results show that expressions of almost all *OsARFs* were
451 reduced in *kxx*, except *OsARF8*, *OsARF10*, *OsARF15*, and *OsARF20* (Figure S9a-d),
452 which suggested that OsLUGL affected floral organ formation and development by
453 regulating the auxin level and signaling pathway.

454

455 **Discussion**

456 Rice is model plant for functional genomics studies in crop plants, its spikelet
457 morphogenesis is important to the achievement of yield. In this study, we identified a
458 mutant *kkx* with unlocked hull phenotype, reduced fertility and bugle in Sp7 palea
459 (Figure 1b and 2m), which indicated that the function of *KKX* in spikelet development.
460 We confirmed that the *KKX* encoded a LUG-like transcriptional regulator. LUG, a
461 member of the Groucho family in *Arabidopsis*, acts as a transcriptional co-repressor
462 to regulate plant development and hormonal signaling (Liu and Meyerowitz, 1995;
463 Conner and Liu, 2000; Sitaraman *et al.*, 2008; Grigorova *et al.*, 2011). LUG to require
464 adaptor protein SEU to form a LUG-SEU complex in order to regulating gene
465 expression (Sridhar *et al.*, 2004). Neither LUG nor SEU possesses a recognizable
466 DNA binding motif, they need AP1 and SEP3 to act as the DNA-binding partners
467 (Gregis *et al.*, 2006; Sridhar *et al.*, 2006; Gregis *et al.*, 2009). Our study demonstrated
468 that OsLUGL also needs to interact with OsSEU to form a complex that acts as a
469 transcriptional regulator (Figure 5a-e), and OsSEU could interacted with SEP3
470 (OsMADS8) and AP1 (OsMADS18) (Figure 5f) to form
471 OsLUGL-OsSEU-OsAP1-OsSEP3 complex in rice.

472 Expression analysis of some floral organ-related genes in wild-type and *kkx* showed
473 that *OsLUGL* acted as a positive regulator of almost all A/B/C/D/E genes. In
474 *Arabidopsis*, there is a ABCDE model of floral organ specification, A-class genes
475 specify the identity of sepals in whorl 1; A- and B-class genes function together
476 determine the identity of petals in whorl 2; B- and C-class genes coordinated define
477 stamen identity in whorl 3; and C- and D-class genes act to specify carpels in whorl 4.
478 E-class genes are co-regulator with A-, B-, C- and D-class genes during floral identity
479 in all whorls (Coen and Meyerowitz, 1991; Alvarez-Buylla *et al.*, 2010; Litt and
480 Kramer, 2010). Previous research has shown that A-class genes and C-class genes
481 function antagonize each other, and LUG represses the expression of *AG* genes
482 (C-class) (Ma and dePamphilis, 2000). There is a similar ABCDE model in rice
483 (Ferrario *et al.*, 2004; Bommert *et al.*, 2005; Thompson and Hake, 2009; Ciaffi *et al.*,

484 2011; Tanaka *et al.*, 2013; Zhang and Yuan, 2014; Wang *et al.*, 2015; Dreni and Zhang,
485 2016). But, in this study, in *kxx*, A-class genes and C-class genes are all
486 down-regulated. We also test their expression in 5 mm young inflorescences, the
487 expression of A-class and C-class genes still down-regulated (Figure S10). These
488 results indicated that OsLUGL-OsSEU might have different role in regulating
489 A/B/C/D gene expression in rice, or there are another unknown factors involved in
490 this regulated process.

491 Previous reports considered that normal development of *mrp* may require *OsMADS1*
492 and *OsMADS6* (Khanday *et al.*, 2013; Tao *et al.*, 2018). Mutation of *OsMADS1*
493 resulted in uncharacteristic flowers and/or loss of flower determinacy, suggesting a
494 role of *OsMADS1* in specifying determinacy of the flower meristem, and effects on
495 development of all floral organs (Hu *et al.*, 2015). An *osmads6* mutant showed defects
496 in palea identity; the palea was half open and likely caused by lack of interlocking
497 between lemma and palea (Ohmori *et al.*, 2009; Li *et al.*, 2010; Tao *et al.*, 2018).
498 Similarly, in *kxx*, the glume was half opened (Figure 1b). Compared with *osmads1*
499 and *osmads6*, the phenotypes of *kxx* were weaker than *osmads1* and similar to
500 *osmads6*. Confusingly, the expression of *OsMADS1* and *OsMADS6* were no
501 significant different between wild-type and *kxx* (Figure 6a-c). So, we suspect there
502 might be another factors or pathway to regulating the floral development in rice.
503 *OsGH3-8* is a downstream target of *OsMADS6* and an auxin negative component in
504 regulating auxin level and activity, and *dsRNAiOsMGH3* line shows the similar
505 phenotype as *kxx* (Yadav *et al.*, 2011). In this study, we confirmed that *OsMADS8* and
506 *OsMADS18* can act as a positive regulator of *OsGH3-8* (Figure 7). Also, the
507 expression of *OsMADS8*, *OsMADS18* and *OsGH3-8* were repressed in *kxx* (Figure 6
508 and 7d). There are 12 members of *GH* in rice, we test the other *OsGH* in *kxx*, most of
509 them were down-regulated except *OsGH3-12* and *OsGH3-13*, but the expression of
510 *OsGH3-12* and *OsGH3-13* were very low (Figure S11). The repressed transcriptional
511 of *OsGH* indicate that *OsMADS8* and/or *OsMADS18*, or the other *OsMADS*-box
512 genes could regulate *OsGH* expression directly, which need to be further studied. All
513 these results show that OsLUGL-OsSEU-OsAP1-OsSEP3 could regulate the *OsGH*

514 transcriptional directly. But, in this study, the reasons for the altered expression of
515 OsMADS8 and OsMADS8 are still unknown. Besides, the level of auxin in *kkx* was
516 increased, which indicate that OsLUGL affect the auxin level, and OsLUGL regulate
517 floral development by auxin relative pathway.

518 Morphogen-like properties in developmental processes, such as meristem
519 specification and lateral organ formation, are often attributed to auxin. These
520 processes are mediated by Aux/IAA induced protein degradation and subsequent
521 *auxin response factor (ARF)* activation (Guilfoyle and Hagen, 2007; Zhang and Yuan,
522 2014; Weijers and Wagner, 2016). Many *ARFs* in *Arabidopsis*, such as *arf1*, *arf2*, and
523 *arf3* are reported to affect floral organs (Ellis *et al.*, 2005; Nishimura *et al.*, 2005;
524 Zheng *et al.*, 2018). We described rice mutant, *osarf19*, in which florets displayed
525 three types of abnormalities. The first was an additional lemma-like organ on the
526 same side as the palea, the second was an enlarged palea with a curved tip, which
527 generated an unclosed floret, and the third was a variably degenerated palea (Zhang *et*
528 *al.*, 2015). In the present study, we assayed expression of *OsARFs* and most of them
529 were down-regulated in *kkx* (Figure S9). This result provides the evidence that the
530 auxin-dependent gene expression relies on the inhibiting role of auxin, as inhibitors of
531 the *ARFs*. So we confirm that OsLUGL regulate floral development by regulate the
532 *OsARFs* expression.

533 In previous study, OsMADS6 interact with OsMADS13, and redundantly regulate
534 carpel/ovule identity and floral determinacy (Li *et al.*, 2011). OsMADS6 was also
535 shown to physically interact with OsMADS4 during early flower development (Seok
536 *et al.*, 2010). Also, in rice flower development, OsMADS1 interact with OsMADS6,
537 and B-, C- and D-class proteins (Hu *et al.*, 2015). So, we suspect that AP1 protein
538 interact with SEP3 protein. We test the interaction of OsMADS8 (SEP3 gene),
539 OsMADS14, OSMADS15 and OsMADS18 (AP1 genes). Yeast two-hybrid assays
540 demonstrated that OsMADS8 physically interacts with OsMADS14, OsMADS15 and
541 OsMADS18, respectively. Also, OsMADS14, OsMADs15 and OsMADS18 could
542 interact with each other in yeast (Figure S12). This result indicated that SEP3 and
543 AP1 could co-regulate the expression of OsGH3-8 by form a complex. And it

544 provides the evidence that the OsMADS8 and OSMADS18 have a superposition
545 effect on regulating *OsGH3-8* (Figure 7c).

546 Collectively, our findings show that OsLUGL acts like a transcriptional regulator in
547 regulating the expression of A-, B-, C-, D-, and E-class genes;
548 OsLUGL-OsSEU-OsAP1-OsSEP3 complex could participate in regulation of flower
549 development by regulation *OsGH* expression directly, and indirectly regulating the
550 auxin level and *OsARFs* expression. SEP3 and AP1 worked together to act as
551 co-regulator in regulate *OsGH3-8* expression. However, there are still unanswered
552 questions. We have no direct evidence to explain the regulate relationship between
553 OsLUGL-OsSEU and *OsMADS8/18*. Why there is no transcription repress in this
554 work? We still have no evidence to explain this issue.

555 Normal floral structure is necessary for seed production and quality. An abnormal
556 floret, even a half-opened hull, with normal pollen fertility causes a significant
557 reduction in seed setting because the opened glume cannot prevent rain or dew from
558 entering the floret during the fertilization and early grain-filling stages. Also, an
559 abnormal floret will not provide an optimum space for seed development, thus
560 causing smaller, malformed seeds with poor color and quality. Hence, investigation of
561 the regulatory mechanisms underlying floral development is necessary for rice
562 breeding and production.

563

564 **Supplementary data**

565 Figure S1. Observation of embryo sac development.

566 Figure S2. Agronomic traits contrast between wild-type and *ktx*.

567 Figure S3. Scanning electron micrographs (SEM) analysis epidermis cells of lemma
568 and palea in wild-type and *ktx*.

569 Figure S4. Gene expression profile of *LOC_Os01g042270*.

570 Figure S5. Alignment of nucleic acid sequence and protein sequence of
571 *LOC_Os01g042260*.

572 Figure S6. Phylogenetic analysis of the LUGL family in 15 plants.

573 Figure S7. The amino acid homology sequence analysis of KKKX.

574 Figure S8. The amino acid homology sequence analysis of OsMADS6, OsMADS8
575 and OsMADS18.

576 Figure S9. Expression levels of rice *ARF* family genes in wild-type and *kkx* young
577 inflorescences (15 mm).

578 Figure S10. Expression levels of floral organ development genes in young
579 inflorescences (5 mm) of wild-type and *kkx*, respectively.

580 Figure S11. Expression levels of rice *GH* family genes in wild-type and *kkx* young
581 inflorescences (15 mm).

582 Figure S12. Analysis of the interaction between OsMADSs genes using yeast
583 two-hybrid assays.

584 Table S1. Primers used in mapping.

585 Table S2. Primers used for vector construction in this study.

586 Table S3. Primers used for real-time PCR analysis.

587

588 **Acknowledgments**

589 We thank the Key Laboratory of Biology, Genetics and Breeding of Japonica Rice in
590 the Mid-lower Yangtze River, Ministry of Agriculture, P.R. China, and Jiangsu
591 Collaborative Innovation Center for Modern Crop Production for support. This
592 research was supported by the National Key Research and Development Program of
593 China (2017YFD0100401), National Key Transform Program (2016ZX08001004)
594 and Jiangsu Science and Technology Development Program (BE2018388).

595

596 **References**

- 597 **Alvarez-Buylla ER, Azpeitia E, Barrio R, Benitez M, Padilla-Longoria P.** 2010. From ABC genes to
598 regulatory networks, epigenetic landscapes and flower morphogenesis: making biological sense of
599 theoretical approaches. *Semin Cell Dev Biol* **21**, 108-117.
- 600 **Arora R, Agarwal P, Ray S, Singh AK, Singh VP, Tyagi AK, Kapoor S.** 2007. MADS-box gene family in rice:
601 genome-wide identification, organization and expression profiling during reproductive development
602 and stress. *BMC Genomics* **8**, 242.
- 603 **Attia KA, Abdelkhalik AF, Ammar MH, Wei C, Yang J, Lightfoot DA, El-Sayed WM, El-Shemy HA.** 2009.
604 Antisense phenotypes reveal a functional expression of OsARF1, an auxin response factor, in

- 605 transgenic rice. *Curr Issues Mol Biol* **11 Suppl 1**, i29-34.
- 606 **Boer DR, Freire-Rios A, van den Berg WA, Saaki T, Manfield IW, Kepinski S, Lopez-Vidriero I,**
607 **Franco-Zorrilla JM, de Vries SC, Solano R, Weijers D, Coll M.** 2014. Structural basis for DNA binding
608 specificity by the auxin-dependent ARF transcription factors. *Cell* **156**, 577-589.
- 609 **Bommert P, Satoh-Nagasawa N, Jackson D, Hirano HY.** 2005. Genetics and evolution of inflorescence
610 and flower development in grasses. *Plant Cell Physiol* **46**, 69-78.
- 611 **Callens C, Tucker MR, Zhang D, Wilson ZA.** 2018. Dissecting the role of MADS-box genes in monocot
612 floral development and diversity. *J Exp Bot* **69**, 2435-2459.
- 613 **Chen J, Gao H, Zheng XM, Jin M, Weng JF, Ma J, Ren Y, Zhou K, Wang Q, Wang J, Wang JL, Zhang X,**
614 **Cheng Z, Wu C, Wang H, Wan JM.** 2015. An evolutionarily conserved gene, FUWA, plays a role in
615 determining panicle architecture, grain shape and grain weight in rice. *Plant J* **83**, 427-438.
- 616 **Ciaffi M, Paolacci AR, Tanzarella OA, Porceddu E.** 2011. Molecular aspects of flower development in
617 grasses. *Sex Plant Reprod* **24**, 247-282.
- 618 **Coen ES, Meyerowitz EM.** 1991. The war of the whorls: genetic interactions controlling flower
619 development. *Nature* **353**, 31-37.
- 620 **Conner J, Liu Z.** 2000. LEUNIG, a putative transcriptional corepressor that regulates AGAMOUS
621 expression during flower development. *Proc Natl Acad Sci U S A* **97**, 12902-12907.
- 622 **Cui R, Han J, Zhao S, Su K, Wu F, Du X, Xu Q, Chong K, Theissen G, Meng Z.** 2010. Functional
623 conservation and diversification of class E floral homeotic genes in rice (*Oryza sativa*). *Plant J* **61**,
624 767-781.
- 625 **Ditta G, Pinyopich A, Robles P, Pelaz S, Yanofsky MF.** 2004. The SEP4 gene of *Arabidopsis thaliana*
626 functions in floral organ and meristem identity. *Curr Biol* **14**, 1935-1940.
- 627 **Dreni L, Kater MM.** 2014. MADS reloaded: evolution of the AGAMOUS subfamily genes. *New Phytol*
628 **201**, 717-732.
- 629 **Dreni L, Pilatone A, Yun D, Erreni S, Pajoro A, Caporali E, Zhang D, Kater MM.** 2011. Functional
630 analysis of all AGAMOUS subfamily members in rice reveals their roles in reproductive organ identity
631 determination and meristem determinacy. *Plant Cell* **23**, 2850-2863.
- 632 **Dreni L, Zhang D.** 2016. Flower development: the evolutionary history and functions of the AGL6
633 subfamily MADS-box genes. *J Exp Bot* **67**, 1625-1638.
- 634 **Ellis CM, Nagpal P, Young JC, Hagen G, Guilfoyle TJ, Reed JW.** 2005. AUXIN RESPONSE FACTOR1 and
635 AUXIN RESPONSE FACTOR2 regulate senescence and floral organ abscission in *Arabidopsis thaliana*.
636 *Development* **132**, 4563-4574.
- 637 **Ferrario S, Immink RG, Angenent GC.** 2004. Conservation and diversity in flower land. *Curr Opin Plant*
638 *Biol* **7**, 84-91.
- 639 **Fornara F, de Montaigu A, Coupland G.** 2010. SnapShot: Control of flowering in *Arabidopsis*. *Cell* **141**,
640 550, 550 e551-552.
- 641 **Gregis V, Sessa A, Colombo L, Kater MM.** 2006. AGL24, SHORT VEGETATIVE PHASE, and APETALA1
642 redundantly control AGAMOUS during early stages of flower development in *Arabidopsis*. *Plant Cell* **18**,
643 1373-1382.
- 644 **Gregis V, Sessa A, Dorca-Fornell C, Kater MM.** 2009. The *Arabidopsis* floral meristem identity genes
645 AP1, AGL24 and SVP directly repress class B and C floral homeotic genes. *Plant J* **60**, 626-637.
- 646 **Grigorova B, Mara C, Hollender C, Sijacic P, Chen X, Liu Z.** 2011. LEUNIG and SEUSS co-repressors
647 regulate miR172 expression in *Arabidopsis* flowers. *Development* **138**, 2451-2456.
- 648 **Guilfoyle TJ, Hagen G.** 2007. Auxin response factors. *Curr Opin Plant Biol* **10**, 453-460.

- 649 **Habets ME, Offringa R.** 2014. PIN-driven polar auxin transport in plant developmental plasticity: a key
650 target for environmental and endogenous signals. *New Phytol* **203**, 362-377.
- 651 **Hiei Y, Ohta S, Komari T, Kumashiro T.** 1994. Efficient transformation of rice (*Oryza sativa* L.) mediated
652 by *Agrobacterium* and sequence analysis of the boundaries of the T-DNA. *Plant J* **6**, 271-282.
- 653 **Hu L, Liang W, Yin C, Cui X, Zong J, Wang X, Hu J, Zhang D.** 2011. Rice MADS3 regulates ROS
654 homeostasis during late anther development. *Plant Cell* **23**, 515-533.
- 655 **Hu Y, Liang W, Yin C, Yang X, Ping B, Li A, Jia R, Chen M, Luo Z, Cai Q, Zhao X, Zhang D, Yuan Z.** 2015.
656 Interactions of OsMADS1 with Floral Homeotic Genes in Rice Flower Development. *Mol Plant* **8**,
657 1366-1384.
- 658 **Ikeda M, Miura K, Aya K, Kitano H, Matsuoka M.** 2013. Genes offering the potential for designing
659 yield-related traits in rice. *Current Opinion in Plant Biology* **16**, 213-220.
- 660 **Kawakatsu T, Yamamoto MP, Touno SM, Yasuda H, Takaiwa F.** 2009. Compensation and interaction
661 between RISBZ1 and RPBF during grain filling in rice. *Plant J* **59**, 908-920.
- 662 **Khanday I, Yadav SR, Vijayraghavan U.** 2013. Rice LHS1/OsMADS1 controls floret meristem
663 specification by coordinated regulation of transcription factors and hormone signaling pathways. *Plant*
664 *Physiol* **161**, 1970-1983.
- 665 **Li H, Liang W, Hu Y, Zhu L, Yin C, Xu J, Dreni L, Kater MM, Zhang D.** 2011. Rice MADS6 interacts with
666 the floral homeotic genes SUPERWOMAN1, MADS3, MADS58, MADS13, and DROOPING LEAF in
667 specifying floral organ identities and meristem fate. *Plant Cell* **23**, 2536-2552.
- 668 **Li H, Liang W, Jia R, Yin C, Zong J, Kong H, Zhang D.** 2010. The AGL6-like gene OsMADS6 regulates
669 floral organ and meristem identities in rice. *Cell Res* **20**, 299-313.
- 670 **Litt A, Kramer EM.** 2010. The ABC model and the diversification of floral organ identity. *Semin Cell Dev*
671 *Biol* **21**, 129-137.
- 672 **Liu Z, Meyerowitz EM.** 1995. LEUNIG regulates AGAMOUS expression in Arabidopsis flowers.
673 *Development* **121**, 975-991.
- 674 **Ma H, dePamphilis C.** 2000. The ABCs of floral evolution. *Cell* **101**, 5-8.
- 675 **Malcomber ST, Kellogg EA.** 2004. Heterogeneous expression patterns and separate roles of the
676 SEPALLATA gene LEAFY HULL STERILE1 in grasses. *Plant Cell* **16**, 1692-1706.
- 677 **Malcomber ST, Kellogg EA.** 2005. SEPALLATA gene diversification: brave new whorls. *Trends Plant Sci*
678 **10**, 427-435.
- 679 **Nelson BK, Cai X, Nebenfuhr A.** 2007. A multicolored set of in vivo organelle markers for
680 co-localization studies in Arabidopsis and other plants. *Plant J* **51**, 1126-1136.
- 681 **Nishimura T, Wada T, Yamamoto KT, Okada K.** 2005. The Arabidopsis STV1 protein, responsible for
682 translation reinitiation, is required for auxin-mediated gynoecium patterning. *Plant Cell* **17**,
683 2940-2953.
- 684 **Ohmori S, Kimizu M, Sugita M, Miyao A, Hirochika H, Uchida E, Nagato Y, Yoshida H.** 2009. MOSAIC
685 FLORAL ORGANS1, an AGL6-like MADS box gene, regulates floral organ identity and meristem fate in
686 rice. *Plant Cell* **21**, 3008-3025.
- 687 **Ohta M, Ohme-Takagi M, Shinshi H.** 2000. Three ethylene-responsive transcription factors in tobacco
688 with distinct transactivation functions. *Plant J* **22**, 29-38.
- 689 **Overvoorde PJ, Okushima Y, Alonso JM, Chan A, Chang C, Ecker JR, Hughes B, Liu A, Onodera C,**
690 **Quach H, Smith A, Yu G, Theologis A.** 2005. Functional genomic analysis of the
691 AUXIN/INDOLE-3-ACETIC ACID gene family members in Arabidopsis thaliana. *Plant Cell* **17**, 3282-3300.
- 692 **Pelaz S, Ditta GS, Baumann E, Wisman E, Yanofsky MF.** 2000. B and C floral organ identity functions

- 693 require SEPALLATA MADS-box genes. *Nature* **405**, 200-203.
- 694 **Pinyopich A, Ditta GS, Savidge B, Liljegren SJ, Baumann E, Wisman E, Yanofsky MF.** 2003. Assessing
695 the redundancy of MADS-box genes during carpel and ovule development. *Nature* **424**, 85-88.
- 696 **Prasad K, Parameswaran S, Vijayraghavan U.** 2005. OsMADS1, a rice MADS-box factor, controls
697 differentiation of specific cell types in the lemma and palea and is an early-acting regulator of inner
698 floral organs. *Plant J* **43**, 915-928.
- 699 **Seok HY, Park HY, Park JI, Lee YM, Lee SY, An G, Moon YH.** 2010. Rice ternary MADS protein
700 complexes containing class B MADS heterodimer. *Biochem Biophys Res Commun* **401**, 598-604.
- 701 **Sitaraman J, Bui M, Liu Z.** 2008. LEUNIG_HOMOLOG and LEUNIG perform partially redundant
702 functions during Arabidopsis embryo and floral development. *Plant Physiol* **147**, 672-681.
- 703 **Sridhar VV, Surendrarao A, Gonzalez D, Conlan RS, Liu Z.** 2004. Transcriptional repression of target
704 genes by LEUNIG and SEUSS, two interacting regulatory proteins for Arabidopsis flower development.
705 *Proc Natl Acad Sci U S A* **101**, 11494-11499.
- 706 **Sridhar VV, Surendrarao A, Liu Z.** 2006. APETALA1 and SEPALLATA3 interact with SEUSS to mediate
707 transcription repression during flower development. *Development* **133**, 3159-3166.
- 708 **Tanaka W, Pautler M, Jackson D, Hirano HY.** 2013. Grass meristems II: inflorescence architecture,
709 flower development and meristem fate. *Plant Cell Physiol* **54**, 313-324.
- 710 **Tao J, Liang W, An G, Zhang D.** 2018. OsMADS6 Controls Flower Development by Activating Rice
711 FACTOR OF DNA METHYLATION LIKE1. *Plant Physiol* **177**, 713-727.
- 712 **Theissen G, Saedler H.** 2001. Plant biology. Floral quartets. *Nature* **409**, 469-471.
- 713 **Thompson BE, Hake S.** 2009. Translational biology: from Arabidopsis flowers to grass inflorescence
714 architecture. *Plant Physiol* **149**, 38-45.
- 715 **Wang H, Zhang L, Cai Q, Hu Y, Jin Z, Zhao X, Fan W, Huang Q, Luo Z, Chen M, Zhang D, Yuan Z.** 2015.
716 OsMADS32 interacts with PI-like proteins and regulates rice flower development. *J Integr Plant Biol* **57**,
717 504-513.
- 718 **Wang K, Tang D, Hong L, Xu W, Huang J, Li M, Gu M, Xue Y, Cheng Z.** 2010. DEP and AFO regulate
719 reproductive habit in rice. *PLoS Genet* **6**, e1000818.
- 720 **Wang Y, Wang C, Zheng M, Lyu J, Xu Y, Li X, Niu M, Long W, Wang D, Wang H, Terzaghi W, Wang Y,
721 Wan J.** 2016. WHITE PANICLE1, a Val-tRNA Synthetase Regulating Chloroplast Ribosome Biogenesis in
722 Rice, Is Essential for Early Chloroplast Development. *Plant Physiol* **170**, 2110-2123.
- 723 **Weijers D, Wagner D.** 2016. Transcriptional Responses to the Auxin Hormone. *Annu Rev Plant Biol* **67**,
724 539-574.
- 725 **Wu D, Liang W, Zhu W, Chen M, Ferrandiz C, Burton RA, Dreni L, Zhang D.** 2018. Loss of LOFSEP
726 Transcription Factor Function Converts Spikelet to Leaf-Like Structures in Rice. *Plant Physiol* **176**,
727 1646-1664.
- 728 **Yadav SR, Khanday I, Majhi BB, Veluthambi K, Vijayraghavan U.** 2011. Auxin-responsive OsMGH3, a
729 common downstream target of OsMADS1 and OsMADS6, controls rice floret fertility. *Plant Cell Physiol*
730 **52**, 2123-2135.
- 731 **Yamamoto Y, Kamiya N, Morinaka Y, Matsuoka M, Sazuka T.** 2007. Auxin biosynthesis by the YUCCA
732 genes in rice. *Plant Physiol* **143**, 1362-1371.
- 733 **Yuan Z, Gao S, Xue DW, Luo D, Li LT, Ding SY, Yao X, Wilson ZA, Qian Q, Zhang DB.** 2009. RETARDED
734 PALEA1 controls palea development and floral zygomorphy in rice. *Plant Physiol* **149**, 235-244.
- 735 **Yun D, Liang W, Dreni L, Yin C, Zhou Z, Kater MM, Zhang D.** 2013. OsMADS16 genetically interacts
736 with OsMADS3 and OsMADS58 in specifying floral patterning in rice. *Mol Plant* **6**, 743-756.

737 **Zahn LM, Kong H, Leebens-Mack JH, Kim S, Soltis PS, Landherr LL, Soltis DE, Depamphilis CW, Ma H.**
738 2005. The evolution of the SEPALLATA subfamily of MADS-box genes: a preangiosperm origin with
739 multiple duplications throughout angiosperm history. *Genetics* **169**, 2209-2223.
740 **Zhang D, Yuan Z.** 2014. Molecular control of grass inflorescence development. *Annu Rev Plant Biol* **65**,
741 553-578.
742 **Zhang J, Nallamilli BR, Mujahid H, Peng Z.** 2010. OsMADS6 plays an essential role in endosperm
743 nutrient accumulation and is subject to epigenetic regulation in rice (*Oryza sativa*). *Plant J* **64**,
744 604-617.

745 **Zhang Q, Xu J, Jiandi, Li Y, Yun.** 2007. Morphological, Anatomical and Genetic Analysis for a Rice. *Journal*
746 *of Genetics and Genomics* **34**, 519-526.
747 **Zhang S, Wu T, Liu S, Liu X, Jiang L, Wan J.** 2015. Disruption of OsARF19 is Critical for Floral Organ
748 Development and Plant Architecture in Rice (*Oryza sativa* L.). *Plant Molecular Biology Reporter*, Vol. 34,
749 748-760.
750 **Zhao Y.** 2010. Auxin biosynthesis and its role in plant development. *Annu Rev Plant Biol* **61**, 49-64.
751 **Zheng Y, Zhang K, Guo L, Liu X, Zhang Z.** 2018. AUXIN RESPONSE FACTOR3 plays distinct role during
752 early flower development. *Plant Signal Behav* **13**, e1467690.
753
754

755 **Figure legend**

756 **Fig. 1** . Phenotypic characteristics of wild-type and *kkx*.

757 (A) Phenotype between wild-type and *kkx* at the post-heading stage. Scale bars = 50
758 cm. (B) Phenotypes of mature seeds with and without seed coat of wild-type and *kkx*.
759 Scale = 5 mm. (C) Spikelets phenotype of wild-type and *kkx* after removal of the
760 palea. Scale bar = 3 mm. (D and E) Comparisons between wild-type and *kkx* in pistils
761 (D) and mature anthers (E). Scale bar = 2 mm. (F and G) Pollen fertility of wild-type
762 and *kkx* observed by staining with 1% I₂-KI. Scale bar = 600 μm.

763

764 **Fig. 2.** Histological analysis of wild-type and *kkx* spikelets.

765 (A and D) Cross sections of spikelets showing five vascular bundles in the lemma
766 (black asterisks) and three vascular bundles in the palea (red asterisks) in wild-type (A)
767 and *kkx* (D). White lines indicate the mrp of paleas in wild-type (A) and *kkx* (D), red
768 brackets indicate the bop of paleas of wild-type (A) and *kkx* (D). Scale bar = 500μm.
769 (B-C and E-F) Cross sections of palea edges in wild-type (B and C) and *kkx* (E and F).
770 Black asterisks indicate vascular bundles in the lemma, and red asterisks indicate
771 vascular bundles in the palea. Scale bar = 300μm. (G-J) Scanning electron

772 micrographs (SEM) analysis of early spikelets of wild-type at different stages. (G)
773 Sp6; (H) early Sp7; (I) Sp7; (J) Sp8. (K-N) Scanning electron micrographs of early
774 spikelets of *kkx* at different stages. (K) Sp6; (L) early Sp7; (M) Sp7; and (N) Sp8.
775 White square indicate the bulge on palea of *kkx*. White asterisks indicate the stamens
776 in wild-type and *kkx* spikelets, respectively. pi, pistils; le, lemma; pa, palea. Scale bar,
777 50 μ m in (G to N).

778

779 **Fig. 3.** Map-based cloning and identification of *KAIKOUXIAO* (*KKX*).

780 (A) *KKX* was preliminarily mapped between markers InterB and RM11322 on
781 chromosome 1. (B) Fine-mapping of the *KKX* locus. *KKX* was positioned on
782 chromosome 1 between BACs OSJNBa0090K04 and P0410E03 within a 36.8 kb
783 region flanked by In-Del markers Y6 and Y10 using 513 mutant individuals. (C)
784 Three predicted open reading frames are located in the 36.8 kb region. (D) Gene
785 structure of candidate gene *LOC_Os01g042260*. Black asterisk and black arrow
786 indicate the position and differing amino acids in wild-type and *kkx*. (E-K)
787 Characterisation of T₀ transgenic plants. Phenotypes of wild-type (E) and *RNAi* line
788 (F) florets at the heading stage. Scale bar = 0.5 mm. (G) Relative expression levels of
789 *LOC_Os01g042260* in spikelets of wild-type and *RNAi* lines were detected by
790 qRT-PCR, with data normalized to *UBQ* levels. Error bars indicate s.e.m. of the mean
791 of 3 replicates. **, $P < 0.01$, Student's *t* test. (H-K) Cross sections of *RNAi-4* (H and J)
792 and *RNAi-6* (I and K) flower, respectively.

793

794 **Fig. 4.** Subcellular localization and expression pattern of OsLUGL.

795 (A) Subcellular localization of OsLUGL protein. Rice protoplast cell expressing
796 OsLUGL-GFP. From left to right: GFP signal of the fusion protein, mCherry with
797 nuclear location gene as a marker, bright field image and merged image. Scale bar, 1
798 mm. (B) Tissue-specific expression pattern revealed by real-time PCR. RNA was
799 isolated from various tissues of wild-type (left). S, seedlings; R, roots; SH, shoots; L,
800 leaves; P, panicles; SP, young spikelets. Right image shows the relative mRNA
801 expression of *OsLUGL* in spikelets at different developmental stages. Error bars

802 indicate s.e.m. of the mean of 3 replicates. (C) In situ hybridization of *OsLUGL*
803 mRNA. Panicle development at early (1 and 3) and late (2 and 4) stages of panicle
804 development. Antisense probe was used as the negative control (5). Scale bars, 1 mm
805 in 1, 2 and 5; 100 μ m in 3; 200 μ m in 4. sm, spikelet meristem; v, vasculature; f, floret;
806 le, lemma; pa, palea.

807

808 **Fig. 5.** Analysis of LUGL transcriptional regulation mechanism

809 (A) Yeast two-hybrid assays. Schematic representations indicate the truncated LUGL
810 proteins as baits used for yeast two-hybrid assays. Different colored rectangles
811 represent different domains of LUGL^{WT} and LUGL^{kkx} proteins. Yeast diploids were
812 grown on agar plates DDO (-Leu/-Trp) and QDO (-Ade/-His/-Leu/-Trp), respectively.

813 (B) Analysis of interaction strength. Yeast diploids co-expressing Gal4 AD-SEU
814 fusions and GAL4 BD- LUGL^{WT} or GAL4 BD- LUGL^{kkx} fusions were grown in
815 selective liquid media to OD₆₀₀ = 1.0. Diploids were titrated (1, 0.1, 0.01; total 5 μ l)
816 and plated on TDO (-His/-Leu/-Trp) and QDO (-Ade/-His/-Leu/-Trp) agar plates for
817 growth. (C) Bimolecular fluorescence complementation (BiFC) assays showing that

818 LUGL interacts with SEU in the nuclei of leaf cells of *Nicotiana benthamiana*.
819 Signals of enhanced yellow fluorescent protein (eYFP) were not detected in
820 corresponding negative controls. ER marker (mCherry ER-rk CD3-959). Scale bar =
821 20 μ m. (D) Diagrams of constructs used for transactivation assays. (E) Transient rice

822 protoplast repression assays using reporter 5 \times UAS GAL4-LUC mixed with
823 35S::RenillaLUC (REN). LUC/REN ratio was used to indicate reporter gene
824 expression and to control transfection efficiency. The effectors in (D) were mixed
825 with the reporter to co-transfect rice protoplasts. Data are means \pm s.e.m. (n=3). **, P

826 < 0.01, Student's t test. (F) Analysis of the interaction between SEU and
827 AP1(OsMADS14/15/18)/SEP1(OsMADS8) genes using yeast two-hybrid assays.
828 Yeast diploids were grown on agar plates DDO (-Leu/-Trp), TDO (-His/-Leu/-Trp)
829 and QDO (-Ade/-His/-Leu/-Trp), respectively.

830

831 **Fig. 6.** The expression level of floral organ development genes in young

832 inflorescences (15 mm) of wild-type and *kkx*, respectively.

833 (A) Expression of A-class genes (*OsMADS14*, *OsMADS15* and *OsMADS18*), B-class
834 genes (*OsMADS2* and *OsMADS16*), C-class genes (*OsMADS3*, *OsMADS58* and *DL*),
835 D-class genes (*OsMADS13*) and *REPI*. (B) Expression of E-class genes (*OsMADS1*,
836 *OsMADS6*, *OsMADS7*, *OsMADS8*, *OsCFO1*, *OsMADS22*, *OsMADS34*, *OsMADS29*
837 and *OsMADS57*). Data are given as means \pm s.e.m. (n=3). * and **, $P < 0.05$ and 0.01 ,
838 respectively, Student's *t* test.

839

840 **Fig. 7.** OsMADSs promote the expression of *OsGH3-8* and change the level of auxin
841 level.

842 (A) Yeast one-hybrid (Y1H) analysis of OsMADS6, OsMADS8, OsMADS18 and
843 *OsGH3-8* promoter., *OsGH3-8* as the bait vector which promoter fragment-fused lacZ
844 reporter, and the prey vectors containing OsMADS6/8/18-fused GAL1 activation
845 domain. Two vectors were co-transformed into EGY48. (B) Diagrams of constructs
846 used for transactivation assays. (C) Transient expression assays of *OsGH3-8*
847 transcriptional activity modulated by OsMADS8, OsMADS18 and
848 OsMADS8+OsMADS18 respectively in rice protoplasts. *pOsGH3-8:LUC* was
849 co-transformed with either the effector or empty vector, as control, into rice
850 protoplasts.. LUC/REN indicating the level of *OsGH3-8* expression activated by the
851 effectors mentioned before. (D) Expression of IAA relative genes. (E) The level of
852 auxin in young inflorescences (15 mm). Data in (C-E) are given as means \pm s.e.m.
853 (n=3). * and **, $P < 0.05$ and 0.01 , respectively, Student's *t* test.

854

Figures

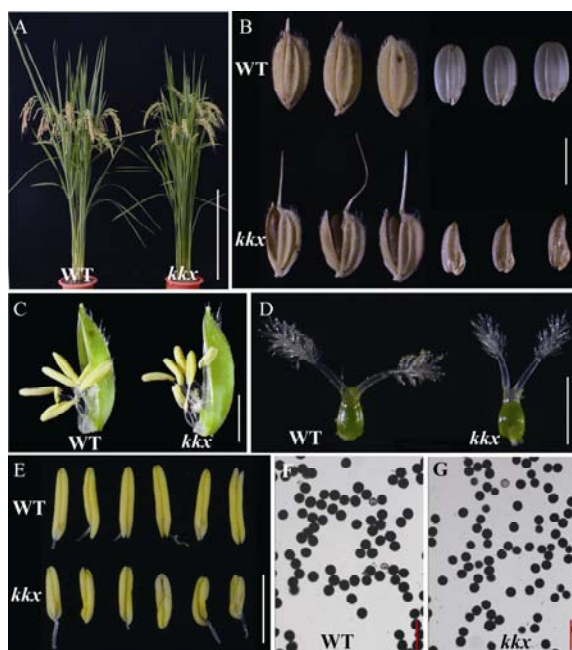


Fig. 1 . Phenotypic characteristics of wild-type and *kcx*.

(A) Phenotype between wild-type and *kcx* at the post-heading stage. Scale bars = 50 cm. (B) Phenotypes of mature seeds with and without seed coat of wild-type and *kcx*. Scale = 5 mm. (C) Spikelets phenotype of wild-type and *kcx* after removal of the palea. Scale bar = 3 mm. (D and E) Comparisons between wild-type and *kcx* in pistils (D) and mature anthers (E). Scale bar = 2 mm. (F and G) Pollen fertility of wild-type and *kcx* observed by staining with 1% I₂-KI. Scale bar = 600 μm.

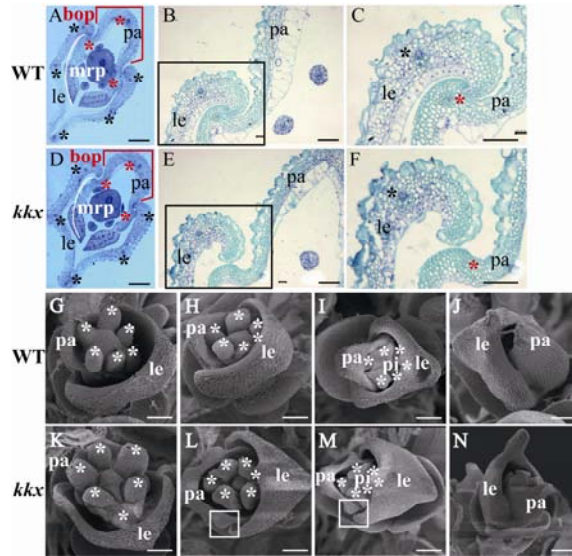


Fig. 2. Histological analysis of wild-type and *kcx* spikelets.

(A and D) Cross sections of spikelets showing five vascular bundles in the lemma (black asterisks) and three vascular bundles in the palea (red asterisks) in wild-type (A) and *kcx* (D). White lines indicate the mrip of paleas in wild-type (A) and *kcx* (D), red brackets indicate the bop of paleas of wild-type (A) and *kcx* (D). Scale bar = 500µm. (B-C and E-F) Cross sections of palea edges in wild-type (B and C) and *kcx* (E and F). Black asterisks indicate vascular bundles in the lemma, and red asterisks indicate vascular bundles in the palea. Scale bar = 300µm. (G-J) Scanning electron micrographs (SEM) analysis of early spikelets of wild-type at different stages. (G) Sp6; (H) early Sp7; (I) Sp7; (J) Sp8. (K-N) Scanning electron micrographs of early spikelets of *kcx* at different stages. (K) Sp6; (L) early Sp7; (M) Sp7; and (N) Sp8. White square indicate the bulge on palea of *kcx*. White asterisks indicate the stamens in wild-type and *kcx* spikelets, respectively. pi, pistils; le, lemma; pa, palea. Scale bar, 50µm in (G to N).

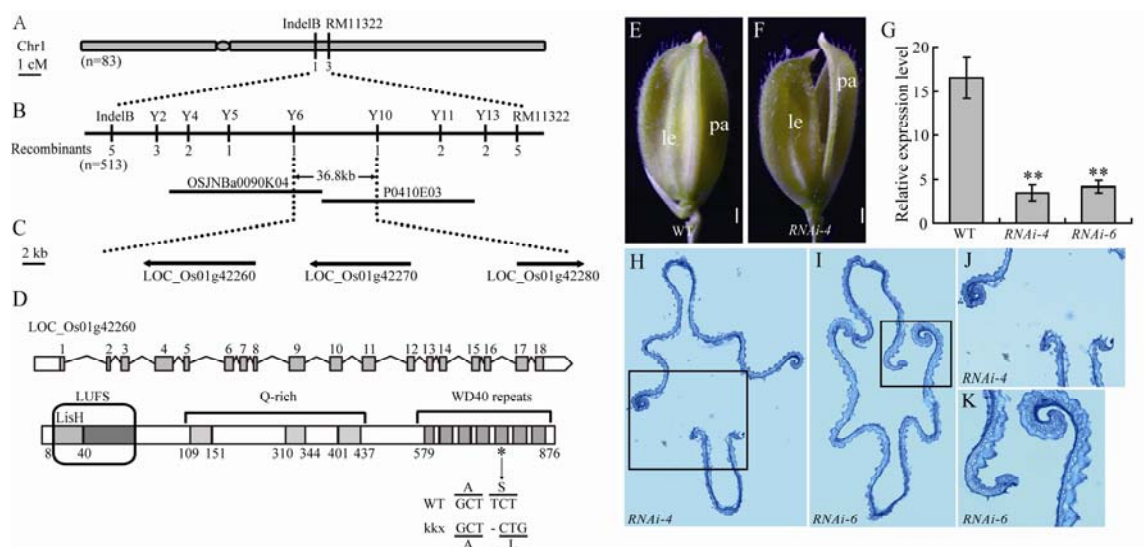


Fig. 3. Map-based cloning and identification of *KAIKOUXIAO* (*KKX*).

(A) *KKX* was preliminarily mapped between markers InterB and RM11322 on chromosome 1. (B) Fine-mapping of the *KKX* locus. *KKX* was positioned on chromosome 1 between BACs OSJNBa0090K04 and P0410E03 within a 36.8 kb region flanked by In-Del markers Y6 and Y10 using 513 mutant individuals. (C) Three predicted open reading frames are located in the 36.8 kb region. (D) Gene structure of candidate gene *LOC_Os01g042260*. Black asterisk and black arrow indicate the position and differing amino acids in wild-type and *kkx*. (E-K) Characterisation of T₀ transgenic plants. Phenotypes of wild-type (E) and *RNAi* line (F) florets at the heading stage. Scale bar = 0.5 mm. (G) Relative expression levels of *LOC_Os01g042260* in spikelets of wild-type and *RNAi* lines were detected by qRT-PCR, with data normalized to *UBQ* levels. Error bars indicate s.e.m. of the mean of 3 replicates. **, $P < 0.01$, Student's *t* test. (H-K) Cross sections of *RNAi-4* (H and J) and *RNAi-6* (I and K) flower, respectively.

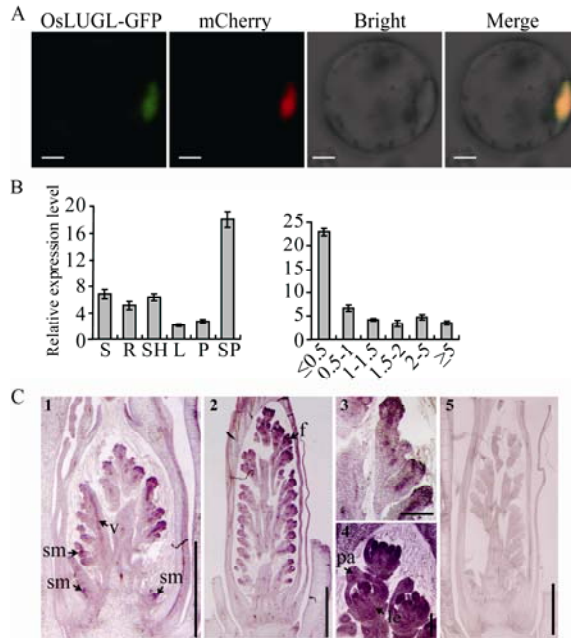


Fig. 4. Subcellular localization and expression pattern of *OsLUGL*.

(A) Subcellular localization of *OsLUGL* protein. Rice protoplast cell expressing *OsLUGL*-GFP. From left to right: GFP signal of the fusion protein, mCherry with nuclear location gene as a marker, bright field image and merged image. Scale bar, 1 mm. (B) Tissue-specific expression pattern revealed by real-time PCR. RNA was isolated from various tissues of wild-type (left). S, seedlings; R, roots; SH, shoots; L, leaves; P, panicles; SP, young spikelets. Right image shows the relative mRNA expression of *OsLUGL* in spikelets at different developmental stages. Error bars indicate s.e.m. of the mean of 3 replicates. (C) In situ hybridization of *OsLUGL* mRNA. Panicle development at early (1 and 3) and late (2 and 4) stages of panicle development. Antisense probe was used as the negative control (5). Scale bars, 1 mm in 1, 2 and 5; 100 μm in 3; 200 μm in 4. sm, spikelet meristem; v, vasculature; f, floret; le, lemma; pa, palea.

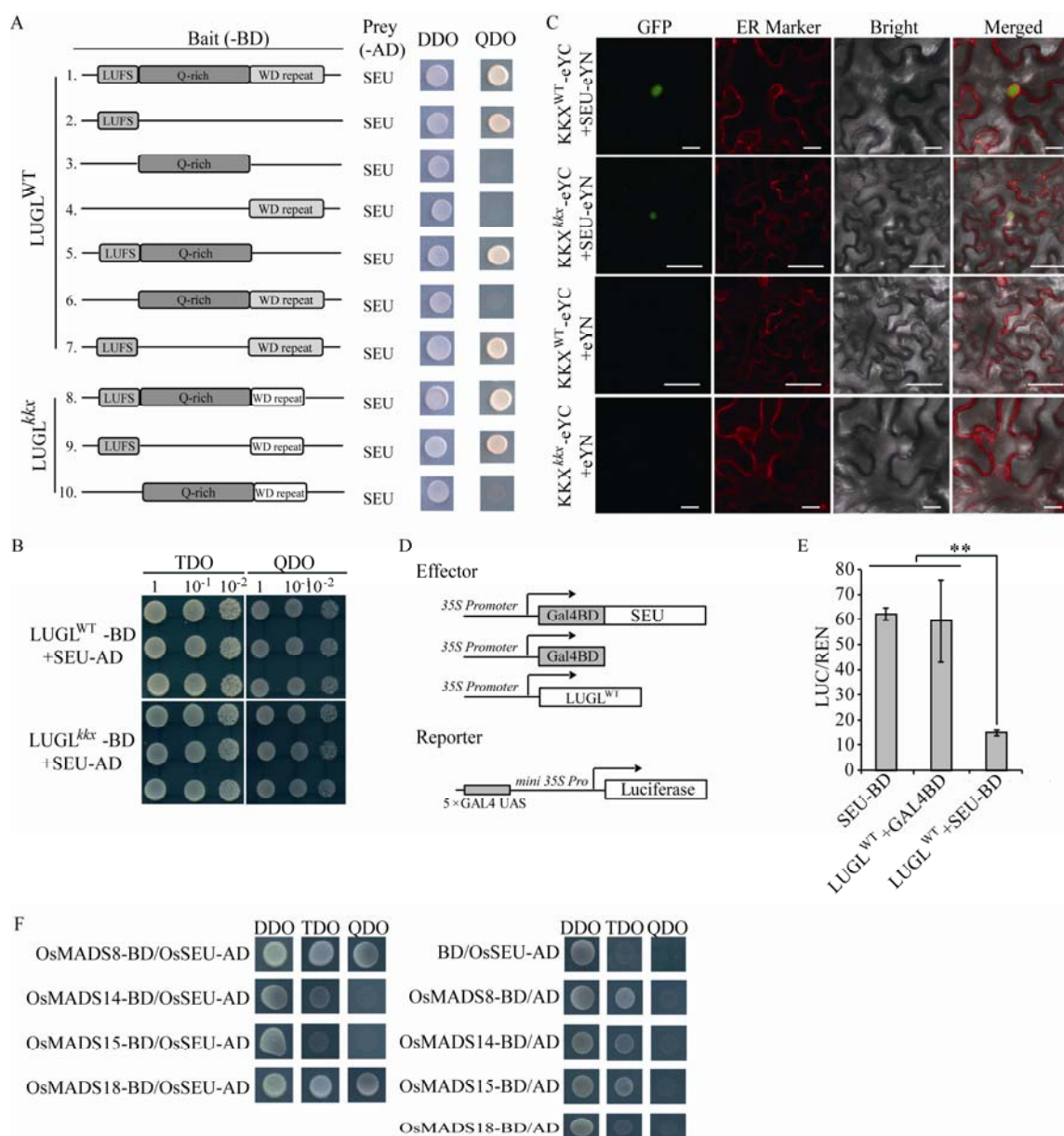


Fig. 5. Analysis of LUGL transcriptional regulation mechanism

(A) Yeast two-hybrid assays. Schematic representations indicate the truncated LUGL proteins as baits used for yeast two-hybrid assays. Different colored rectangles represent different domains of LUGL^{WT} and LUGL^{kkx} proteins. Yeast diploids were grown on agar plates DDO (-Leu/-Trp) and QDO (-Ade/-His/-Leu/-Trp), respectively.

(B) Analysis of interaction strength. Yeast diploids co-expressing Gal4 AD-SEU fusions and GAL4 BD- LUGL^{WT} or GAL4 BD- LUGL^{kkx} fusions were grown in selective liquid media to OD600 = 1.0. Diploids were titrated (1, 0.1, 0.01; total 5 μ l)

and plated on TDO (-His/-Leu/-Trp) and QDO (-Ade/-His/-Leu/-Trp) agar plates for growth. (C) Bimolecular fluorescence complementation (BiFC) assays showing that LUGL interacts with SEU in the nuclei of leaf cells of *Nicotiana benthamiana*. Signals of enhanced yellow fluorescent protein (eYFP) were not detected in corresponding negative controls. ER marker (mCherry ER-rk CD3-959). Scale bar = 20 μ m. (D) Diagrams of constructs used for transactivation assays. (E) Transient rice protoplast repression assays using reporter 5 \times UAS GAL4-LUC mixed with 35S::RenillaLUC (REN). LUC/REN ratio was used to indicate reporter gene expression and to control transfection efficiency. The effectors in (D) were mixed with the reporter to co-transfect rice protoplasts. Data are means \pm s.e.m. (n=3). **, $P < 0.01$, Student's t test. (F) Analysis of the interaction between SEU and AP1(OsMADS14/15/18)/SEP1(OsMADS8) genes using yeast two-hybrid assays. Yeast diploids were grown on agar plates DDO (-Leu/-Trp), TDO (-His/-Leu/-Trp) and QDO (-Ade/-His/-Leu/-Trp), respectively.

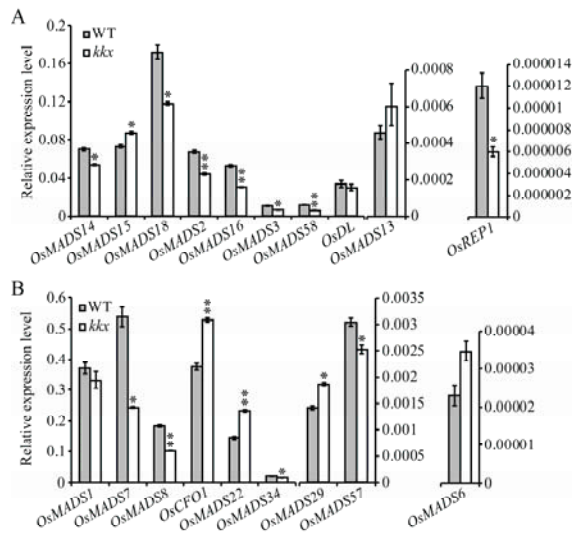


Fig. 6. The expression level of floral organ development genes in young inflorescences (15 mm) of wild-type and *ktx*, respectively.

(A) Expression of A-class genes (*OsMADS14*, *OsMADS15* and *OsMADS18*), B-class genes (*OsMADS2* and *OsMADS16*), C-class genes (*OsMADS3*, *OsMADS58* and *DL*), D-class genes (*OsMADS13*) and *REP1*. (B) Expression of E-class genes (*OsMADS1*, *OsMADS6*, *OsMADS7*, *OsMADS8*, *OsCFO1*, *OsMADS22*, *OsMADS34*, *OsMADS29* and *OsMADS57*). Data are given as means \pm s.e.m. (n=3). * and **, $P < 0.05$ and 0.01 , respectively, Student's *t* test.

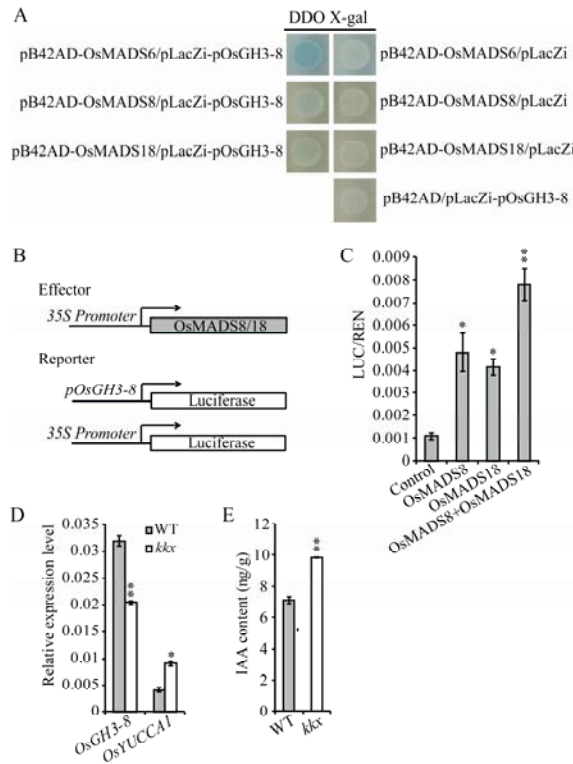


Fig. 7. OsMADSs promote the expression of *OsGH3-8* and change the level of auxin level.

(A) Yeast one-hybrid (Y1H) analysis of OsMADS6, OsMADS8, OsMADS18 and *OsGH3-8* promoter., *OsGH3-8* as the bait vector which promoter fragment-fused lacZ reporter, and the prey vectors containing OsMADS6/8/18-fused GAL1 activation domain. Two vectors were co-transformed into EGY48. (B) Diagrams of constructs used for transactivation assays. (C) Transient expression assays of *OsGH3-8* transcriptional activity modulated by OsMADS8, OsMADS18 and OsMADS8+OsMADS18 respectively in rice protoplasts. *pOsGH3-8*:LUC was co-transformed with either the effector or empty vector, as control, into rice protoplasts. LUC/REN indicating the level of *OsGH3-8* expression activated by the effectors mentioned before. (D) Expression of IAA relative genes. (E) The level of auxin in young inflorescences (15 mm). Data in (C-E) are given as means \pm s.e.m. (n=3). * and **, P<0.05 and 0.01, respectively, Student's *t* test.